

Osteoporosis Detection and Classification on Femur Images

¹Kumari Shilpa,

Assistant Professor, Computer Science and Engineering

²Dr Shubhangi D C

Professor, Computer Science and Engineering

Abstract

Osteoporosis is one of the common bone diseases that reduces bone strength and affects the structure of the bone and thereby increases the chances of fracture risk, more likely in the spine, hip, and wrist. The diagnosis of osteoporosis is done by measuring the bone quality and bone mass, mainly bone mineral density (BMD). There are various methods available to measure the BMD. Of which, Dual Energy X-ray Absorptiometry (DEXA) is considered as the benchmark method. BMD is a parameter to determine the important score known as *T*-score that determines the osteoporosis condition. BMD measurement is visualized in X-ray images and DEXA images. The main objective of the proposed system is femur segmentation. Accurate segmentation will support accurate BMD calculation, and better BMD calculation can strengthen the diagnosing capability of DXA machines.

Keywords- Bone Mineral Density (BMD), Dual Energy X-ray Absorptiometry (DEXA), *T*-score, SVM Classifier.

I. Introduction

Osteoporosis is a systemic skeletal disorder characterized by decreased bone mass and qualitative alterations (macro- and micro-architecture, bone material properties) associated with increased fracture risk. Primary osteoporosis is defined as osteoporosis occurring after menopause (postmenopausal osteoporosis) or with advancing age (senile osteoporosis). Secondary osteoporosis is caused by a number of disorders and drugs. Bone densitometry allows quite accurate and precise measurement of bone mass, particularly its mineral density [bone mineral density (BMD)] in g/cm² of projected bone area. BMD accounts for 60 to 80% of bone mechanical resistance.

According to the World Health Organization (WHO), a densitometric diagnosis of osteoporosis should be based on BMD measured by dual-energy x-ray absorptiometry (DXA), compared to the mean BMD in young normal adults of the same sex (peak bone mass). The unit of measurement is the standard deviation (SD) above or below the mean peak bone mass (*T*-score). It has been reported that fracture risk begins to increase exponentially at a *T*-score < -2.5 SD, which has been established by the WHO as the cut-off for diagnosing osteoporosis. Bone densitometry is therefore the diagnostic test for osteoporosis and fracture risk assessment, just as blood pressure measurement is used to diagnose arterial hypertension and assess the risk of stroke. Though BMD is only one facet responsible for increased fragility, dual x-ray absorptiometry (DXA) measurements of BMD have been universally adopted as a standard to define osteoporosis.

While BMD measured by means of DXA is the standard and state-of-the-art technique for quantifying osteoporosis, research has targeted bone quality as a parameter or biomarker, which provides information on susceptibility to fracture beyond that, provided by BMD and may be used as an outcome measurement for pharmaceutical trials. Multiple innovative imaging techniques have been developed that use radiologic techniques to characterize bone architecture.

DXA, introduced to clinical routine in 1987, is a well-standardized and easy to use technique that has a high precision (maximum acceptable precision error, 2%–2.5%) and low radiation dose (1– 50 mSv, if performed with vertebral fracture assessment) and is currently the best established method to measure BMD in vivo. By using two x-ray beams with differing peak kilovoltage (30–50 and .70 keV) that allow it to subtract the soft tissue component, DXA measures areal BMD typically of the lumbar spine, proximal femur, and distal radius. With an automatic segmentation, which is checked and corrected by the operator at the spine and proximal femur, the L1–4 vertebral bodies, femoral neck, intertrochanteric and trochanteric regions are measured. The total femur region of interest is derived from femoral neck, intertrochanteric, and trochanteric regions. In addition to areal density values in grams per square centimeter, DXA provides *T* scores and *Z* scores. *Z* scores are standard deviations compared with an age-matched reference population, while *T* scores are standard deviations compared with a young adult reference population.

II. Literature Survey

Ling Wang et al. [01] presented an algorithm to denoise medical X-ray images using multiwavelet multiple resolution analysis (MRA) with covariance shrink (CS) method. The proposed system works as: First, the shifted image is pre-filtered into multiple streams. Thresholds are calculated by using the covariance shrink (CS) method. Next, the bivariate soft thresholding is applied to the wavelet coefficients. After which the image is post processed. Finally, the result is inverse transformed. The proposed method was compared with other methods such as Bayes Shrink in wavelet domain and traditional wavelet method.

Mikhaylichenko et al. [02] introduced a method to detect bone delineation in an automatic way. It is based on accurate boundary fragments detection and by eliminating discontinuities between them with further chaining them to contours. The method was tested for X-ray images of various regions in different axial views with various resolutions.

Ying Chen et al. [03] proposed a model-based approach to automatically extract femur contours from hip x-ray images. The first prominent features such as parallel lines in the shaft region and circles in the femoral heads are detected. The model is then refined by active contour algorithm to get results accurately. The authors show that this method can depict the contours in the bone with regular shapes, in spite of size and shape.

Feng Ding et al. [04] explain atlas-based approach for automatic segmentation. A new correlation method is used for segmentation based on the end parts. A local processing happens due to the local refining to derive the envelope. Experimental results show that the proposed algorithm shows good accuracy.

M.G. Roberts et al. [05], proposed linked active appearance models (AAMs) to automatically segment lumbar vertebrae on digitized radiographs us. Digitized lumbar radiographs are used in this study. The results showed the possibility of considerably automating vertebral morphometric measurements on radiographs.

Hassani et al. [06] developed a novel method based on texture features. Retinex algorithm is used for the preprocessing and anisotropic morlet wavelet is used. Then, the anisotropic textures are described using renyi entropy. Renyi entropy is an entropy model used for image thresholding. Neural Network classifier is used for classification based on the extracted features. On enhancing the image, better features are extracted that improves the results of osteoporosis detection.

Pal et al [07] used simple plain digital radiograph of calcaneus to detect osteoporosis. In this work, canny edge detection was performed and the total numbers of both white and black pixels present in trabeculae of calcaneum were calculated. Features were extracted using texture analysis and Grey Level Co-occurrence Matrix (GLCM). BMD was also measured in the right proximal femur using DEXA.

Kiattisin Supapom et al. [08] presented a method for measuring the volume of the bone. Computer-aided method is used for segmenting the needed region. A basic ground model is defined based on expert input. The process involves pre-processing, edge detection method to derive the boundary regions. The delineation is done for the automatic segmentation.

III. Methodology

The accurate diagnosis of osteoporosis from DXA imaging depends on precise image segmentation and ROI extraction. In this paper, we manually select ROIs and segment the femur region and by extracting features we calculate BMD. A general overview of our CAOD model is given in Figure 1 shows proposed system architecture; DXA images are considered as input images. In the preprocessing, the images are resized and de-noised. The preprocessed images are segmented, to segment the ROI, boundary-based, and active shape model applied. The segmented region is considered for feature extraction. The HE, LE, and BMD features are considered. The trained features are classified using the SVM classifier.

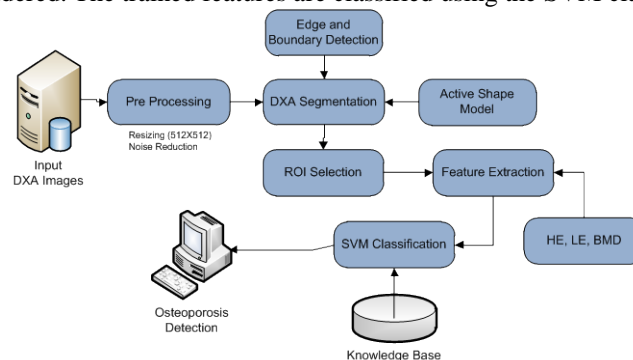


Figure 1: Architecture of the Proposed System.

3.1 Pre-processing

Pre-processing involves the image enhancement by removing the noise for further analysis of the image. Noise is an inherent feature of every medical imaging modality, and it reduces the resolution of and contrast in an image. Thereby, it profoundly affects the diagnostic value and image analysis capability of imaging modalities. To improve the accuracy of image segmentation, noise reduction in both high-energy (HE) and lowenergy (LE) images is an essential preprocessing procedure. For denoising, we used a non-local mean filter, which eliminates noise by comparing the similarity of patches across pixel neighborhoods. The detector and source noises of a DXA system were modeled for both HE and LE DXA images. Different smoothing parameters were used to denoise HE and LE images. The optimized non-local mean filter was tested and verified with DXA images of a uniform femur phantom and real human femur images.

3.2 ROI Selection

DXA Image was first rotated and the femoral shaft axis was standardised to obtain a uniform alignment of the images. Then the region of interest (ROI) measuring 128 X 128 pixels was placed and manually cropped by a trained operator at the clinically significant area on the neck region of each image. The ROIs quantified are typically the total, femoral neck, trochanter, intertrochanter and Ward’s regions. The total femur and femoral neck regions are commonly used for diagnosis, and the trochanter and Ward’s triangle regions are seldom used except for research. The proposed system with a marked ROI on a sample image is outlined in Figure 2(a) and detailed regions are shown in detail in Figure 2(b).

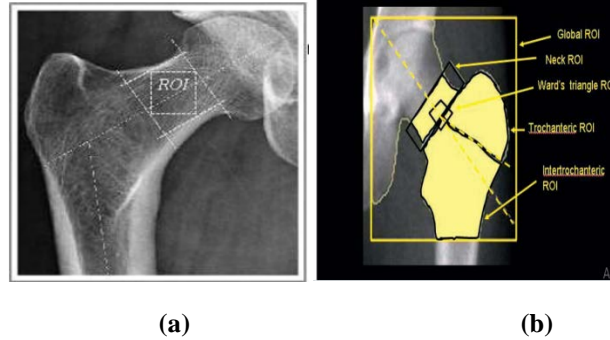


Figure 2 ROI Selection (a) Marked ROI (b) Detailed Regions.

3.3 Segmentation

The femur bone parts are segmented by using Active Shape Model (ASM) image segmentation. T-score value of BMD of each femur bone parts is measured from the segmented region, which is used to diagnose the Osteoporosis. Figure 9 shows the boundary detection for femur bone from the image. Finally, the accuracy between normal X-ray and DEXA scan is compared. The BMD measured from this method correlated well with the values from DEXA.

Active Shape Model (ASM)

K-way and hierarchical segmentation is common segmentations after spectral clustering. K-way perform recursive two-way cut by KMC for partitioning the image. However, this causes incorrect segmentation. Hierarchical segmentation finds non-overlapped regions by oriented watershed transform (OWT), resulting ultra metric contour but this consumes time as whole image is searched and it is infeasible.

ASM captures global information where at the training side all bone contours features are aligned. First, manual segmentation on ROI is done. The landmarks results from segmentation are represented by boundary. 10 points are sampled among successive landmarks. The landmarks counted by operator ranging between 92 to 150. The iterative method (closest point) and affine transformation aligns existing contour with newly contour. The training set includes N training contours described in Eq. (1)

$$S = \{C^a | a \in \{1, \dots, N\}\} \quad (1)$$

Each contour $C^a \in S$ consist set of landmark points $X^a \in C^a$, where $X^a \in C^a$, where

$$X^a = \{c_n^a | n \in \{1, \dots, M\}\} \quad (2)$$

Where

$$c_n^a = (x_n^a, y_n^a) \quad (3)$$

represent coordinates of n' th landmark in C_a . Once training shapes are aligned, mean shape is calculated by

$$S = \{C^a | a \in \{1, \dots, N\}\} \quad (4)$$

Where

$$\bar{c}_n = (\bar{x}_n - \bar{y}_n) \quad (5)$$

$$\bar{x}_n = \left(\frac{1}{k}\right) \sum_a x_m^a \quad (6)$$

$$\bar{y}_n = \left(\frac{1}{k}\right) \sum_a y_m^a \quad (7)$$

where K depicts number of points.

$$X = \bar{x} + \Phi_s b \quad (8)$$

Where \bar{x} is the mean model $\Phi_s = (\Phi_1, \Phi_2, \dots, \Phi_m)$ (9)
 shows eigenvectors matrix similar to m largest eigenvalues λ_i obtained from covariance matrix,

$$s = \left[\frac{1}{(n-1)}\right] \sum_{i=1}^n (x_i - \bar{x})(x_i - \bar{x})^T \quad (10)$$

m is a smallest number giving 99% variance. Eigenvectors, Φ_i , are orthogonal describing points to move when shape varies. Eigenvalue λ_i similar to variance defined by linear deformation. The shape parameter model b is defined as

$$b = \phi_s^T (x - \bar{x}) \quad (11)$$

1.4 Feature Extraction

- HE is the first feature map from DXA. The information of DXA image affected from attenuation. An X-ray beam of HE consist huge penetration in contrast to LE. HE is less useful with less boundaries in bone and soft tissue with contrast to LE.
- LE defines second feature map from DXA. Tissues increases X-ray noise by reducing X-ray energy resulting effective image than HE image.
- Osteoporosis is measured by BMD technique using threshold which is characterised by Gaussian distribution of bone density. BMD defines ratio of bone mineral content (BMC) by scan image area.

$$BMD = \frac{BMC}{area(g/cm^2)} \quad (12)$$

3.5 SVM Classifier

SVM is the best-known member of the kernel methods, which is the class of algorithms for pattern analysis. In SVM, kernel based instance method is adopted. Instead of knowing several fixed parameters of input features, i -th training example (x_i, y_i) and corresponding weights w_i are learned. K define kernel between training x_i and unlabelled input x^1 . Typically binary classifier calculates weighted of the sum of similarities given in the Eq. (13).

$$\hat{y} = sgn \sum_{i=1}^n w_i y_i k(x_i, x') \quad (13)$$

Where $y' \in \{-1, +1\}$ is the kernel binary classifier, $k: X \times X \rightarrow \mathcal{R}$ is the kernel function which measures the similarity among two inputs $x, x' \in X$, $w_i \in \mathbb{R}$ are weights of the training sample, and sgn indicated sign, which concludes classification outcome is positive or negative.

Algorithm: SVM Classification

Input: Samples - training samples, $M \times N$, (a row of column vectors);

Output: Classified Output Type

- Step.1: Kernel: (default: 2)
 0 defines Linear
 1 indicate Polynomial(Gamma)
 2 shows RBF(exponential Gamma)
 3 defines Sigmoid
- Step.2: Default 3
- Step.3: If input is 0, Gamma set to $1/(\max_pattern_dimension)$
 . If input is not 0, Gamma default set to 1
- Step.4: Default 0
- Step.5: Cost of constrain violation for C-SVC, epsilon-SVR, and nu-SVR (default 1)
- Step.6: Cache Size: Space to hold the elements of $K(\langle X(:,i), X(:,j) \rangle)$ matrix (default 40MB)
- Step.7: epsilon: tolerance of termination criterion (default: 0.001)
- Step.8: SVM Type: (default: 0)
 0 defines c-SVC
 1 indicate nu-SVC

- 2 shows one-class SVM
- 3 defines epsilon-SVR
- 4 defines nu-SVR

Step.9: nu-SVC-one-class SVM and nu-SVR (default: 0.5)
 loss tolerance: epsilon-SVR (default: 0.1)

Step.10: Shrinking heuristics, 0 or 1 (default: 1)

Step.11: Weight a row vector or scalar.

Step.12: Outputs: AlphaY- Alpha * Y. Alpha depicts non-zero Lagrange Coefficients, and Y shows Labels, (L-1) x sum(nSV).

- i in AlphaY(j-1, start_Pos_of_i:(start_Pos_of_i+1)-1),
- j in AlphaY(i, start_Pos_of_j:(start_Pos_of_j+1)-1)

Step.13: SVs - Support Vectors. (Sample corresponding the non-zero Alpha),
 M x sum(nSV),]

Step.14: Bias-Bias of all the 2-class classifier(s), 1 x L*(L-1)/2;

Step.15: Parameters - Output parameters of training;

Step.16: nSV – SVs numberfor each class, 1xL;

Step.17: nLabel - Each class Labels, 1xL.

Step.18: The above parameters are passed to SVMClass function to get the decision value and labels output.
 [Labels, DecisionValue]= SVMClass(Samples, AlphaY, SVs, Bias, Parameters, nSV, nLabel);

End algorithm

IV. Experimental Results

The T score is the primary diagnostic value used for osteoporosis as in the elderly, post-menopausal women and men over 50 years, the T score is inversely related to fracture risk. A T score is the difference between the patient's aBMD and a young reference aBMD in units of the population SD. Since the report of the WHO study group published in 1994 , the ISCD has been one of several organizations developing guidelines for scan interpretation based on the use of T scores and Z scores . The T score was first introduced in the late 1980s and is defined as:

$$T_{score} = \frac{aBMD_{patient} - aBMD_{youngAdultMean}}{SD_{youngAdultMEasn}} \quad (14)$$

SD is the standard deviation of the population of young adults. aBMD can also be expressed as a Z score, the difference between the patient's aBMD and an age and typically ethnicity matched reference aBMD and SDs: $Z_{score} =$

$$= \frac{aBMD_{patient} - aBMD_{age,ethnicity-matchedadultmean}}{SD_{age,ethnicity-matchedadultmean}} \quad (15)$$

The T score is used to diagnose osteoporosis in older adults while the Z score is used to diagnose low bone mass in young adults and children. A frequent presumption is that the T and Z scores should be very similar or identical for younger individuals. T and Z-score results obtained from DXA segmentation. ROI and BMD measurement respectively is depicted in Figure 3.

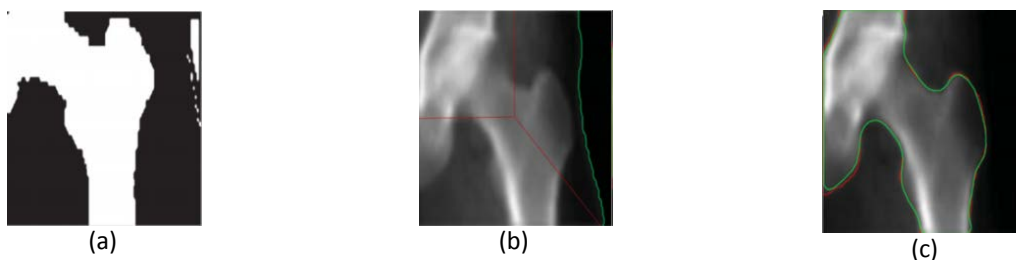


Figure 3: DEXA femur image (a) output (b) segmentation by parts (c) boundaries (green) compared with ground truth (red).

DXA Reports

An automatic summary of the T-score and Z-score reports was generated after some steps such as automatic DXA image as shown in Figure 4. Clinicians should be provided with sufficient information and guidance with DXA reporting so that the most informed and knowledgeable decisions can be made. A patient report with a Tscore > -1.0 is considered normal, and a T-score between -1.0 and -2.5 indicates osteopenia. Meanwhile, a T-score < -2.5 means the patient is considered to have osteoporosis.

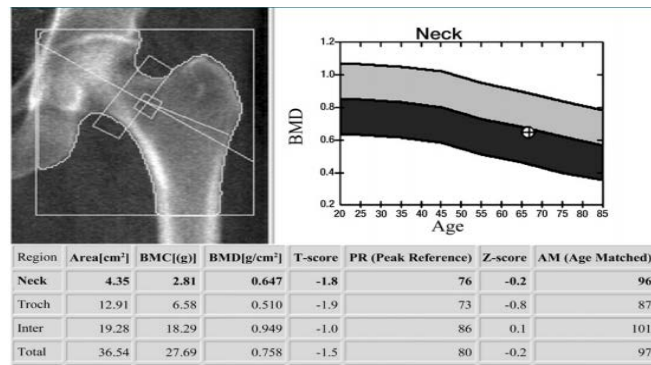


Figure 4: In the proximal femur of a 66-yearold woman, the lowest T score of total and femoral neck regions of interest is used to classify the bone as normal, osteopenic, or osteoporotic. In this postmenopausal woman the T score was 21.8, which is in the osteopenic range.

V. Conclusions

Osteoporosis is a severe skeletal disease caused by lower BMD, which causes an increased risk of bone fracture. DXA is the gold standard used in diagnosing osteoporosis, and various factors impact osteoporosis. In this paper, we proposed a CAOD model featuring ROI selection followed by DXA image segmentation, BMD analysis, and the generation of an osteoporosis report to bring consistency to the process of calculating BMD measurements, thus yielding higher accuracy. The ROI selection results showed that our method has achieved a high level of accuracy of 98.4% when it was tested on more than 20 images. The BMD measurement results from our automatic ROI selection method show a higher degree of accuracy and consistency compared to standard calculations.

References

- [1] J. Lu, L. Wang, Y. Li, and T. Yahagi, "Noise removal for medical X-ray images in multiwavelet domain," *Int. J. Image. Graph.*, Vol. 8, no. 01, pp. 25–46, Jan 2008.
- [2] Mikhaylichenko, Y. Demyanenk, and E. Grushko. "Automatic detection of bone contours in X-ray images." *InAIST (Supplement)*. pp. 212–23. 2016.
- [3] Y. Chen, X. Ee, W. K. Leow, and T. S. Howe. "Automatic extraction of femur contours from hip x-ray images." *International Workshop on Computer Vision for Biomedical Image Applications*, Springer, Berlin, Heidelberg, 2005, pp. 200–9.
- [4] Feng "Application of covariance matrices and wavelet marginals." *arXiv:1410.2663*, 2014.
- [5] M. G. Roberts, T. F. Cootes, and J. E. Adams. "Vertebral shape: Automatic measurement with dynamically sequenced active appearance models." *Proceedings of International Conference on Medical Image Computing and Computer-Assisted Intervention*, 2005, pp. 733–40. Springer, Berlin, Heidelberg.
- [6] E. Hassani, J. El Hassouni, M. Rziza, and E. Lespessailles. "Texture analysis for trabecular bone X-ray images using anisotropic morlet wavelet and Rényi entropy." *Proceedings of the International Conference on Image and Signal Processing*; Springer, Berlin, Heidelberg, 2012, pp. 290–7
- [7] B. Pal, and M. Anburajan. "Digital image processing of calcaneum X-ray in the evaluation of osteoporosis in women: A comparison with DXA bone densitometer as a 'standard'." *Proceedings of the International conference on Electronics and Communication Systems*, 2016, pp. 1865–9.
- [8] K. Supaporn, and C. Kosin. "Femur bone volumetric estimation from a single X-ray image for osteoporosis diagnosis." *International Symposium on Communications and Information Technologies*, Oct. 2006, pp. 1149–52.
- [9] S. N. Fathima, R. Tamilselvi, and M. P. Beham. "DEXSIT: A benchmark database for BMD measurement and analysis." *Proceedings of Fourth International Conference on Biosignals, Images and Instrumentation (ICBSII)*, Mar 2018, pp. 206–12.
- [10] J. J. Carey, and M. F. Delaney. "T-scores and Z-scores," *Clin. rev. bone miner. metab.*, Vol. 8 no. 3, pp. 113–21, Sep. 2010.
- [11] J. W. Kwon, S. I. Cho, Y. B. Ahn, and Y. M. Ro. "Noise reduction in DEXA image based on system noise modeling." *Proceedings of International Conference on Biomedical and Pharmaceutical Engineering*, Dec 2009, pp. 1–6.
- [12] M. A. Al-antari, et al. "Non-local means filter denoising for DEXA images." *Proceedings of 39th Annual International Conference of the IEEE Engineering in Medicine and Biology Society (EMBC)*, Jul 2017, pp. 572–5.